RESEARCH ARTICLE

Strain-modulated bulk photovoltaic effect in negative piezoelectrics

Yue Gao[1], Wenli Zou[1], Jian Zhou[2,*], Chunmei Zhang[1,3,#]

[1]School of Physics, Northwest University, Xi'an 710127, China
[2]Center for Alloy Innovation and Design, State Key Laboratory for Mechanical Behavior of Materials, Xi'an Jiaotong University, Xi'an 710049, China
[3]Shaanxi Key Laboratory for Theoretical Physics Frontiers, Xi'an 710127, China
Corresponding authors. E-mail: *jianzhou@xjtu.edu.cn, #chunmeizhang@nwu.edu.cn
Received December 19, 2025; accepted March 27, 2026

Supplemental Material

I. Tight-binding model of 1D chain

The simple 1D model has two ions in a unit cell. The formal charges of them are ±Z, and at the equilibrium structure, their interatomic bond distances are denoted as R_1 and R_2, giving lattice constant of $L = R_1 + R_2$. To simulate their ionic interactions, we adopt spring-like potential, described by spring stiffness coefficients k_1 and k_2, respectively. Equal separation structure is considered as the referenced structure with zero polarization. Under a nonzero distance mismatch $\eta = R_2 - R_1$, net polarization occurs, which is contributed from ionic and electronic parts separately. In the following, we breakdown their contributions and estimate their effects on the sign of piezoelectric coefficient $d = \frac{\delta P}{\delta \varepsilon}$. Here, ε represents a uniaxial strain along the chain, defined as $\varepsilon = \frac{L'-L}{L}$, where L' and L are the lattice constants in the strained and equilibrium states. The ionic part contribution can be written as

$$P_{\text{ion}} = \frac{1}{L}\left(-Z \times -\frac{\eta}{2}\right) = \frac{Z\eta}{2L} \tag{S1}$$

Under a strain, the new lattice constant $L' = R_1' + R_2'$. At such a new equilibrium structure, it is clearly that $\frac{R_1'-R_1}{R_2'-R_2} = \frac{k_2}{k_1}$. Hence, we can estimate the piezoelectric constant as

$$\begin{aligned} d_{\text{ion}} &= \frac{\delta P_{\text{ion}}}{\delta \varepsilon} = Z\frac{\frac{\eta'}{2L'} - \frac{\eta}{2L}}{L'-L}L = \frac{ZL}{2(L'-L)}\frac{(L'-L)\left(-\eta + \frac{k_1-k_2}{k_1+k_2}L\right)}{LL'} \\ &= \frac{Z}{2L'}\frac{[-\eta(k_1+k_2) + L(k_1-k_2)]}{k_1+k_2} = \frac{Z}{2L'}\frac{[-\eta(k_1+k_2) + L(k_1-k_2)]}{k_1+k_2} \\ &= \frac{Z}{(k_1+k_2)L'}(R_1k_1 - R_2k_2) \end{aligned} \tag{S2}$$

Therefore, the sign of $\frac{\delta P_{\text{ion}}}{\delta \varepsilon}$ is determined by two factors, the formal charge Z and the relative magnitude between equilibrium distance $\frac{R_2}{R_1}$ and stiffness $\frac{k_1}{k_2}$.

Next, we discuss the electronic polarization P_{el}. As described in the main text, we adopt a two-orbital spinless tight-binding model

$$H = -\frac{t}{2}\sum_n \left(c_n^\dagger c_{n+1} + c_{n-1}^\dagger c_n\right) + \frac{\Delta}{2}\sum_n (-1)^i c_n^\dagger c_n \tag{S3}$$

Here, t is the hopping integral between nearest neighbor ions, and $\pm\frac{\Delta}{2}$ is their on-site energies. Giving $\beta = \left|\frac{t}{\Delta}\right| \ll 1$, the eigenenergies take the form of

$$E_{\pm}(k) = \pm\frac{\Delta}{2}\sqrt{1+16\beta^2\cos^2\frac{kL}{2}} \simeq \pm\frac{\Delta}{2}\left(1+8\beta^2\cos^2\frac{kL}{2}\right) \tag{S4}$$

It opens a direct band gap ($E_g = \Delta$) at the X point. Through $(H(k) - E(k)I)\psi(k) = 0$, the conduction band Bloch wave function are derived as:

$$|u_+(k)\rangle = \frac{1}{\sqrt{N_+(k)}}\begin{pmatrix} -\beta g(k)\Delta \\ \frac{\Delta}{2}\left(1-\sqrt{1+4\beta^2|g(k)|^2}\right)\end{pmatrix} \tag{S5}$$

And the valence band Bloch wave function is:

$$|u_-(k)\rangle = \frac{1}{\sqrt{N_-(k)}}\begin{pmatrix} -\beta g(k)\Delta \\ \frac{\Delta}{2}\left(1+\sqrt{1+4\beta^2|g(k)|^2}\right)\end{pmatrix} \tag{S6}$$

where $g(k) = e^{-iR_1k} + e^{iR_2k} = 2e^{i\frac{\eta}{2}k}\cos\frac{Lk}{2}$, and $\sqrt{N_\pm(k)}$ is the normalization factor.

Perform a Taylor expansion about β: $|u_-(k)\rangle \simeq \begin{pmatrix} -\beta g(k) + O(\beta^3) \\ 1 + O(\beta^2)\end{pmatrix} \simeq \begin{pmatrix} -\beta g(k) \\ 1\end{pmatrix}$.

This gives

$$i\left\langle u_-(k)\left|\frac{d}{dk}\right|u_-(k)\right\rangle = i\beta^2 g^*(k)\frac{dg(k)}{dk} \tag{S7}$$

Here,

$$g^*(k) = 2e^{-i\frac{\eta}{2}k}\cos\frac{Lk}{2} \tag{S8}$$

$$\frac{dg(k)}{dk} = e^{i\frac{\eta}{2}k_x}\left(i\eta\cos\left(\frac{Lk_x}{2}\right) - Lsin\left(\frac{Lk_x}{2}\right)\right) \tag{S9}$$

$$|g(k)|^2 = 4cos^2\frac{Lk}{2} \tag{S10}$$

$$\frac{d}{dk}|g(k)|^2 = -4L\cos\left(\frac{Lk_x}{2}\right)sin\left(\frac{Lk_x}{2}\right) \tag{S11}$$

Then, we can obtain

$$ig^*(k)g'(k) = -2\eta cos^2\frac{Lk}{2} - 2iL\cos\left(\frac{Lk_x}{2}\right)sin\left(\frac{Lk_x}{2}\right) \tag{S12}$$

$$\begin{aligned} P_{\text{el}} &= \frac{ie}{2\pi}\int_{-\frac{\pi}{L}}^{\frac{\pi}{L}}\left\langle u_-(k)\left|\frac{d}{dk}\right|u_-(k)\right\rangle dk = \frac{ie}{2\pi}\int_{-\frac{\pi}{L}}^{\frac{\pi}{L}}\beta^2 g^*(k)g'(k)dk \\ &= -\frac{e\beta^2\eta}{4\pi}\int_{-\frac{\pi}{L}}^{\frac{\pi}{L}}|g(k)|^2\,dk + \frac{e\delta^2}{2\pi}\frac{i}{2}\int_{-\frac{\pi}{L}}^{\frac{\pi}{L}}\frac{d}{dk}|g(k)|^2\,dk \\ &= -\beta^2\frac{e\eta}{L} + O(\beta^3) \end{aligned} \tag{S13}$$

Here, we expand the expression according to the power of unit-less parameter β. One sees that the polarization is zero when the two sites are equally separated ($\eta = 0$), consistent with previous assumption. Since $P_{\text{el}} \propto \frac{1}{L}$, the tensile (compressive) strain could reduce (enhance) the magnitude of $|P_{\text{el}}|$. Performing derivative, we have

$$d_{\mathrm{el}} = \frac{\delta P_{\mathrm{el}}}{\delta \varepsilon} = -\beta^2 e \frac{\frac{\eta'}{L'} - \frac{\eta}{L}}{L' - L} L = \frac{-\beta^2 e L}{L' - L} \frac{(L' - L)\left(-\eta + \frac{k_1 - k_2}{k_1 + k_2} L\right)}{LL'} = \frac{-\beta^2 e}{L'} \frac{[-\eta(k_1 + k_2) + L(k_1 - k_2)]}{k_1 + k_2}$$
$$= \frac{-2\beta^2 e}{(k_1 + k_2)L'} (R_1 k_1 - R_2 k_2) \qquad (S14)$$

Therefore, the sign of $\frac{\delta P_{\mathrm{el}}}{\delta \varepsilon}$ is also determined by the relative magnitude between equilibrium distance $\frac{R_2}{R_1}$ and stiffness $\frac{k_1}{k_2}$. Note that we assume a constant hopping integral t in the model, which is only approximately correct under small strain. Nevertheless, as $P_{\mathrm{el}} \propto \beta^2$, the electron contributed polarization (and the piezoelectric coefficient) is order of magnitude smaller than the ion contributions P_{ion}.

We assume $Z > 0$, under the condition of $\frac{k_1}{k_2} < \frac{R_2}{R_1}$, this model exhibits a negative piezoelectric response. Then, we assume specific TB parameters to realize the negative piezoelectricity. Building upon reported negative piezoelectric materials [S1, S2] with negative longitudinal piezoelectric coefficients, we choose suitable atomic distances (R_1 = 1.5 Å and R_2 = 2.2 Å). The relationship between "stiff" k_1 and "soft" k_2 should satisfy $k_1 \frac{R_1}{R_2} < k_2$. In addition, to maintain a clear distinction between the "stiff" and "soft" regions, we consider $k_2 < k_1$. These two criteria are sufficient conditions for the negative piezoelectricity in the 1D chain model. Here, we take a representative value of $k_1 = 1.2k_2$ to perform our analysis. Note that this specific choice would not affect the main physical conclusion of this work. t_0 is the hopping constant between the nearest neighbor, which is set to be 0.2 eV. Collectively, these parameters conform to the requirement $\frac{\delta P}{\delta \varepsilon} < 0$ and successfully demonstrate negative piezoelectricity, as shown in Table S1. Note that to capture the strain-dependent evolution of nonlinear optical response, a decay length r_0 of 1.433 Å was incorporated for the hopping parameter when shift current is calculated. Here, the hopping parameter are evaluated by $t_i(R_i) = t_0 \exp\left(-\frac{R_i - R_0}{r_0}\right)$.

TABLE S1. The strain ($\varepsilon = (L' - L)/L$), the lattice parameters (L'), the distance mismatch (η), the polarization magnitude P_{ion}, P_e, and P_{tot}, band gap, and the largest peak value of σ^{xxx} of 1D chain under strain in the negative piezoelectric regime.

ε	L'(Å)	η(Å)	P_{ion} (10^{-2} e/Å)	P_e (10^{-3} e/Å)	P_{tot} (e/Å)	Band gap (eV)	σ^{xxx} (μA/V^2)
–2%	3.626	0.694	9.55	7.65	0.1033	1.0123	16.675
–1 %	3.663	0.697	9.50	7.60	0.1027	1.0121	16.564
0%	3.700	0.700	9.45	7.57	0.1021	1.0119	16.438
1%	3.737	0.703	9.41	7.53	0.1016	1.0117	16.296
2%	3.774	0.706	9.36	7.49	0.1011	1.0115	16.139

Furthermore, based on the above derivation, the condition for realizing a positive piezoelectric response can be correspondingly obtained as $k_1 > \frac{R_2}{R_1} k_2$. Within the same parameter framework, stiffness coefficients satisfying this condition are adopted to model the shift current response in positive piezoelectric materials. As a representative case, we choose $k_2 = 0.5\, k_1$ to investigate the behavior. One sees that tensile strain concurrently increases polarization and shift vector, yielding an enhanced shift current component.

TABLE S2. The strain ($\varepsilon = (L' - L)/L$), the lattice parameters (L'), the distance mismatch (η), the polarization magnitude P_{ion}, P_e, and P_{tot}, band gap, and the largest peak value of σ^{xxx} of 1D chain under strain in the positive piezoelectric regime.

ε	L'(Å)	η(Å)	P_{ion} (10^{-2} e/Å)	P_e (10^{-3} e/Å)	P_{tot} (e/Å)	Band gap (eV)	σ^{xxx} (μA/V^2)
–2%	3.626	0.694	9.27	7.41	0.1000	1.0115	16.210
–1 %	3.663	0.697	9.36	7.49	0.1011	1.0117	16.334
0%	3.700	0.700	9.46	7.57	0.1021	1.0119	16.441
1%	3.737	0.703	9.55	7.64	0.1032	1.0121	16.533
2%	3.774	0.706	9.65	7.77	0.1042	1.0122	16.608

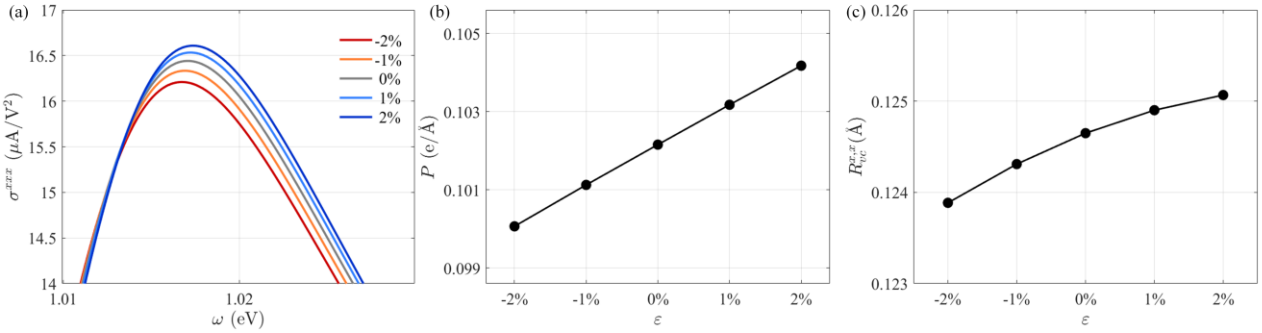

Figure S1 (a) Shift current photoconductance, (b) polarization and (c) shift vector at X points of the 1D chain TB model under strain (ε = –2% ~ 2%) in the positive piezoelectric regime.

TABLE S3. Comparison of electric polarization *P*, BPVE response evolution for positive and negative piezoelectrics under compressive strain. The symbols ↑ (↓) denote increase (decrease) trends under strain, respectively.

	materials	Compressive strain	
		P	BPVE response
negative piezoelectrics	r-GeX	↑	↑
	group-V monolayers[S3]	↑	↑
positive piezoelectrics	2H-MoS_2[S4]	↓	↓
	3R-MoS_2[S5]	↓	↓

II. Electronic structure of r-GeTe

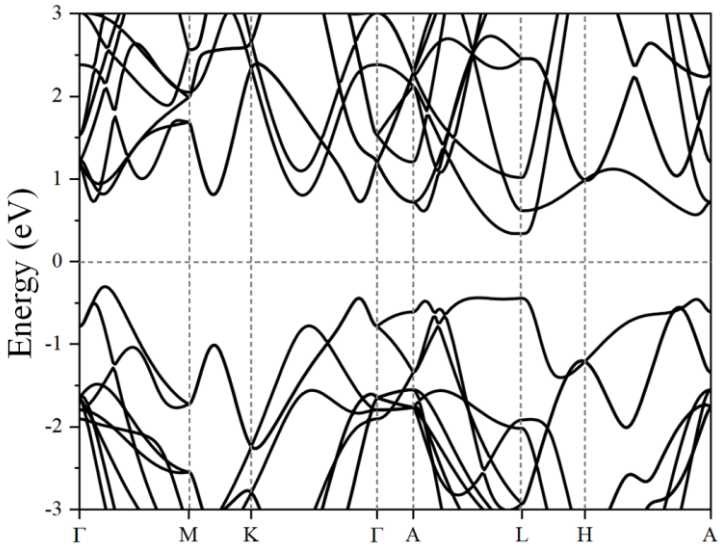

Figure S2. Calculated band structure without spin-orbit coupling (SOC) of r-GeTe.

III. The resolved shift current of r-GeTe

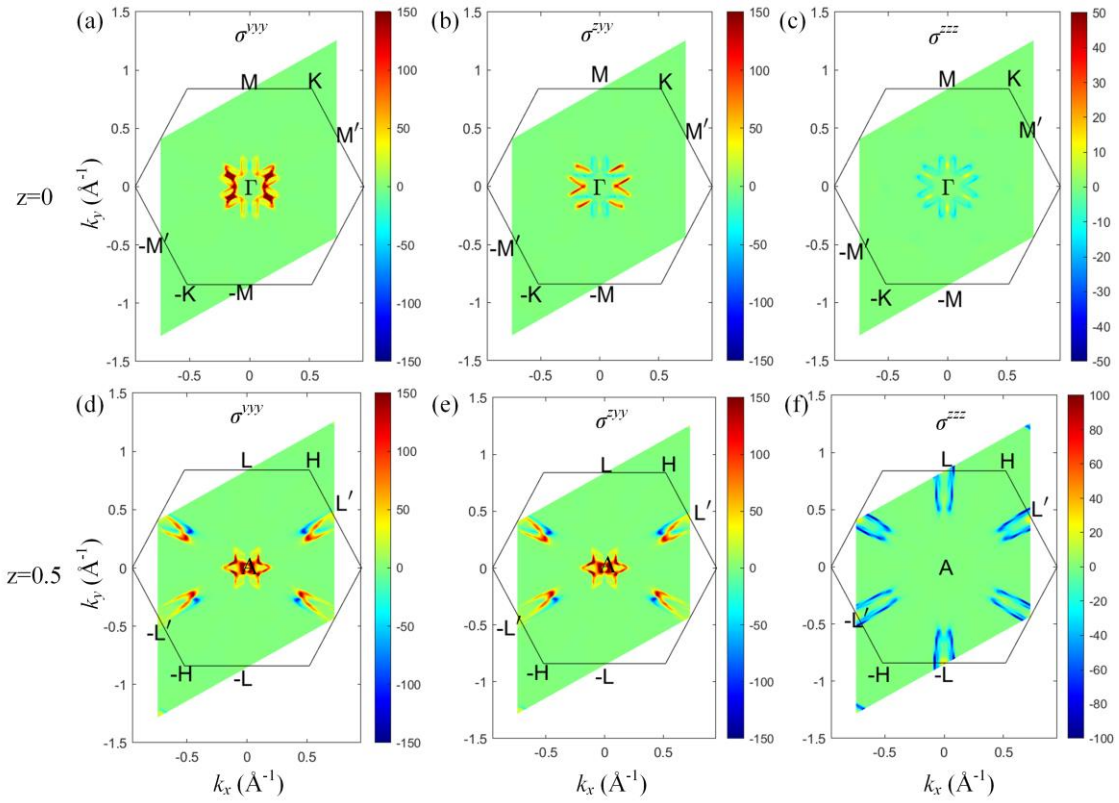

Figure S3. The *k*-resolved shift current conductance σ^{yyy}, σ^{zyy}, and σ^{zzz} in the first Brillouin zone (BZ) of the bulk r-GeTe at $k_z = 0\times\pi/c$, $k_z = 0.5\times\pi/c$.

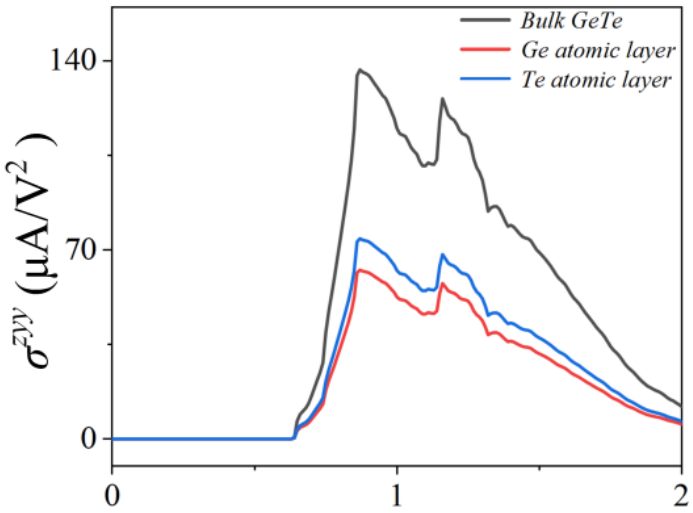

Figure S4. The calculated σ^{zyy} photoconductivity on the Ge atomic layer and Te atomic layer.

IV. *k*-resolved shift vector and r_{mn} of r-GeTe under strain

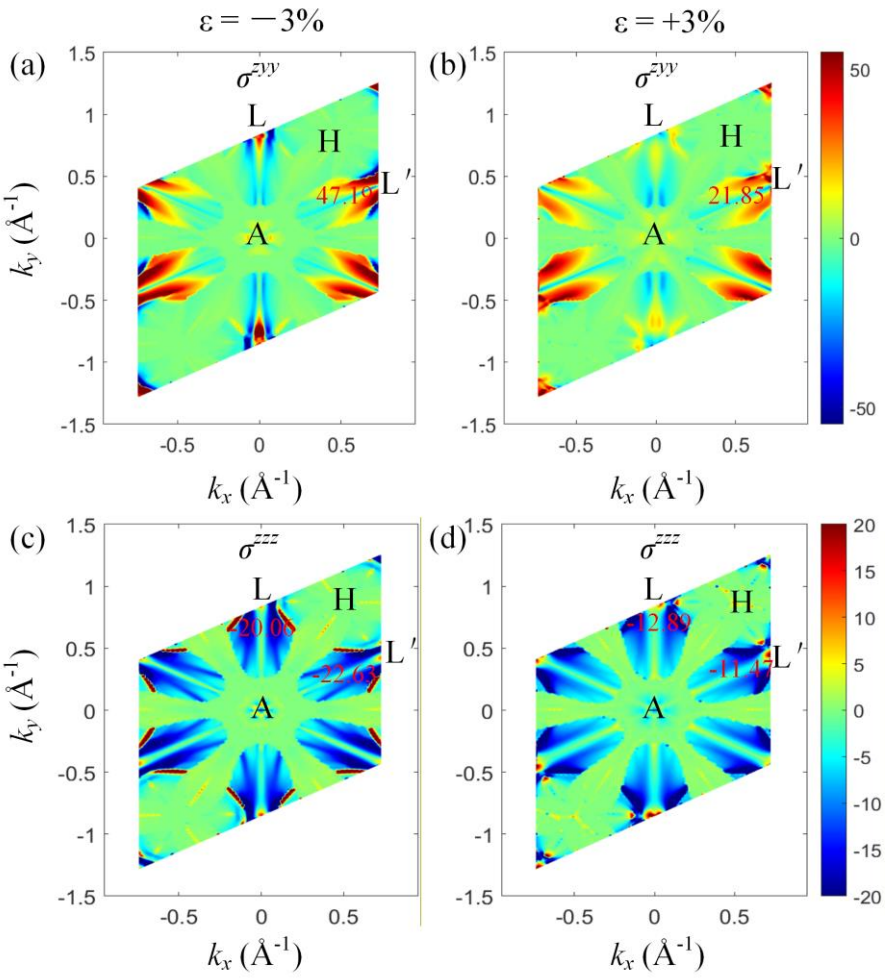

Figure S5. *k*-resolved shift vector of σ^{zyy} and σ^{zzz} in the first BZ between the valence band maximum (VBM) and the conduction band minimum (CBM), CB-2 of r-GeTe under out-of-plane strain (ε = −3%, 3%) at $k_z = 0.5\times\pi/c$. The typical values around L and L′points (0.5, 0, 0.5) for all cases are marked in each panel, which are (a) 47.19 Å, (b) 21.85 Å, (c) −20.06 Å, −22.63 Å, (d) −12.89 Å, −11.47 Å, respectively. One sees that the shift vector exhibits a larger magnitude under compressive strain compared to tensile strain.

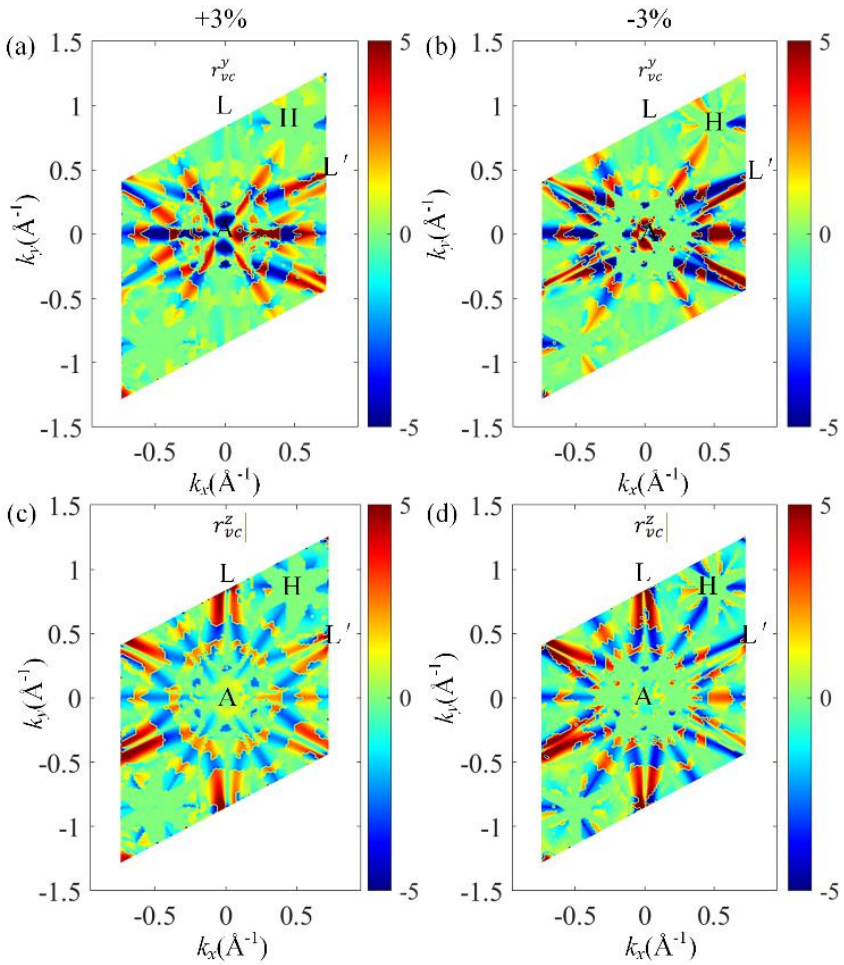

Figure S6 The interband Berry connection r_{vc}^{y} and r_{vc}^{z} of r-GeTe in the BZ between the top valence band and bottom conduction band under ±3% strain, at $k_z = 0.5\times\pi/c$. The typical values of r_{vc}^{y} around the L′ point (0.5, 0, 0.5) for the cases are (a) 2.15 Å, (b) 5.23 Å, and that of r_{vc}^{z} around the L point (0, 0.5, 0.5) for the cases are (c) 1.76 Å, (d) 4.66 Å, respectively. One sees that the interband Berry connection r_{vc}^{y} and r_{vc}^{z} exhibit a larger magnitude under compressive strain compared to the tensile strain.

TABLE S4 The *s*-, *p*-orbital weight of Ge and Te atoms in VBM and CBM.

	Band	Ge-*s*	Ge-p_y	Ge-p_z	Ge-p_x	Te-*s*	Te-p_y	Te-p_z	Te-p_x
-3%	VBM	0.112	0.012	0.107	0.012	0.024	0.080	0.114	0.025
	CBM	0.018	0.104	0.073	0.104	0.031	0.043	0.059	0.044
+3%	VBM	0.169	0.005	0.071	0.005	0.073	0.008	0.203	0.008
	CBM	0.002	0.170	0.020	0.170	0.005	0.036	0.008	0.036

V. The shift current of r-GeTe under strain

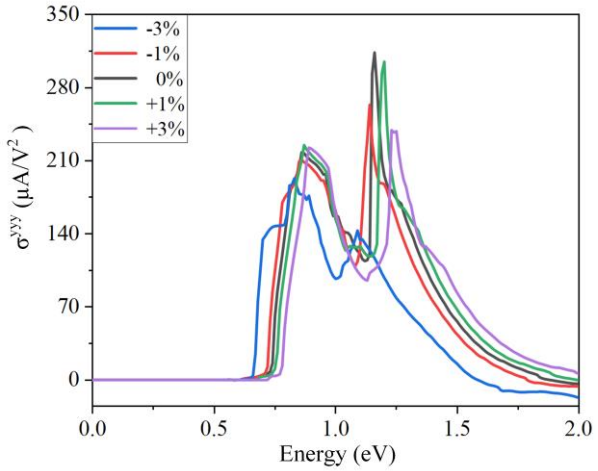

Figure S7. Shift current conductance σ^{yyy} of the bulk r-GeTe under out-of-plane strain.

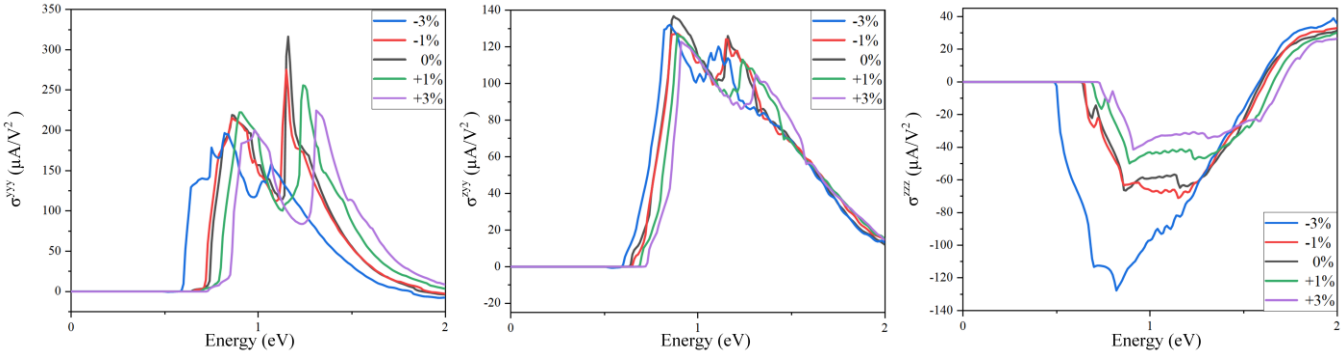

Figure S8. Shift current conductance (a) σ^{yyy}, (b) σ^{zyy}, and (c) σ^{zzz} of the bulk r-GeTe under in-plane biaxial strain.

VI. The shift current of r-GeX (X=S, Se)

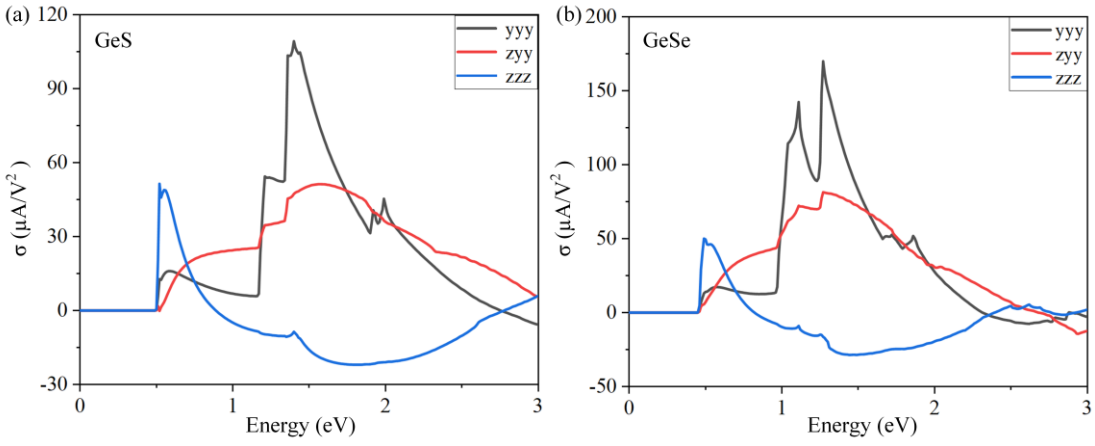

Figure S9. Shift current conductance of the bulk rhombohedral (a) GeS and (b) GeSe.

References

[S1] L. You, Y. Zhang, S. Zhou, A. Chaturvedi, S. A. Morris, F. Liu, L. Chang, D. Ichinose, H. Funakubo, W. Hu, T. Wu, Z. Liu, S. Dong, J. Wang, Origin of giant negative piezoelectricity in a layered van der Waals ferroelectric, Sci. Adv. 5(4), eaav3780 (2019).

[S2] Y. Liu, W. Wang, Z. Wang and C. Si, Ultrahigh Negative Longitudinal Piezoelectricity in Rhombohedral GeTe and Its Group IV–VI Analogues, Nano Lett. 25(9), 3630 (2025).

[S3] F. Xu, H. Su1, Z. Gong, Y Wei, H Jin and H. Guo, Controllable ferroelectricity and bulk photovoltaic effect in elemental group-V monolayers through strain engineering, Phys. Rev. B 106(19), 195418 (2022)

[S4] W. Wang, Y. Xiao, T. Li, X. Lu, N. Xu, Y. Cao, Piezo-photovoltaic Effect in Monolayer 2H-MoS_2, J. Phys. Chem. Lett. 15(13), 3549 (2024).

[S5] Y. Dong, M. M. Yang, M. Yoshii, S. Matsuoka, S. Kitamura, T. Hasegawa, N. Ogawa, T. Morimoto, T. Ideue and Y. Iwasa, Giant bulk piezophotovoltaic effect in 3R-MoS_2, Nat. Nanotechnol 18(1032), 36 (2023).